Depth detection and image recovery in remote sensing by optical scanning holography

Taegeun Kim
Sejong University
Department of Optical Engineering
98 Kunja-Dong, Kwangjin-Ku
Seoul, 143-747, Korea

Ting-Chung Poon
Virginia Polytechnic Institute and State University (Virginia Tech)
Optical Image Processing Laboratory
Bradley Department of Electrical and Computer Engineering
Blacksburg, Virginia 24061

Guy Indebetouw
Virginia Polytechnic Institute and State University (Virginia Tech)
Physics Department
Blacksburg, Virginia 24061

Abstract. We propose an algorithm that can extract the depth location of a target from its complex hologram directly in optical remote sensing applications. The target is located in a 3-D space and its complex hologram is obtained by optical scanning holography. Once the target's depth has been extracted, we can recover the image of the target from its hologram.
[DOI: 10.1117/1.1476939]

Subject terms: depth detection; three-dimensional rotation- and scale-invariant pattern recognition; optical scanning holography; optical remote sensing.

Paper 010237 received July 6, 2001; accepted for publication Nov. 9, 2001.

1 Introduction

Optical correlation techniques have a long-standing history and have been shown to be very useful for two-dimensional (2-D) pattern recognition and target tracking in 2-D applications.[1,2] Optical 2-D correlation matches the image of a target object and that of a reference object and gives the 2-D location of the matched object[3–5] and, therefore, it is restricted to pattern recognition and target tracking in 2-D space. There are increasing interests in image recognition and target tracking in three-dimensional (3-D) space because the actual world is 3-D and a target is located in the actual 3-D space.[6–8] Recently, the use of holographic information was proposed to represent 3-D objects for optical image recognition and target location in 3-D space.[9–12] The location of a matched object is based on the 2-D correlation of the holographic information of the 3-D target object and that of the 3-D reference object. The correlation data is then analyzed by the Wigner distribution to extract the depth location of the matched target. If the target object is not matched with the reference object, however, one cannot obtain the depth location of the target in three dimensions.

In this paper, we investigate a technique that extracts the depth location of a target directly from its complex hologram (or a single-sideband hologram). Once the depth location is extracted, we can reconstruct the target image. This reconstructed 2-D image then can be recognized using standard rotation- and distortion-invariant 2-D optical correlation techniques,[13–15] which gives the 2-D location of the target. Thus, one can achieve rotation- and distortion-invariant recognition as well as depth detection in 3-D space.

We first acquire the complex hologram of the target using optical scanning holography. Optical scanning holography is a real-time holographic recording technique in which the complex hologram of a 3-D object is obtained as an electrical signal by 2-D optical scanning of the 3-D object.[16] Section 2 briefly reviews optical scanning holography and discusses ways in which the complex hologram of a target can be generated by 2-D scanning of the target. As it turns out, if we analyze the spectra of the complex hologram, the target's phase spectrum contains two pieces of information: depth information and the target's phase spectrum. The two spectra are blended together and this makes it difficult to extract the depth location of the target directly from the complex hologram. In Sec. 3, we propose an algorithm that can extract the depth information directly from the complex hologram. In a spectral domain, we will first synthesize something called a real-only spectrum hologram. We then propose a filter to extract the depth location of the target from the real-only spectrum hologram. The filtered output is further analyzed by the Wigner distribution, which eventually gives the depth location of the target on a space-frequency map. With the extracted depth information, we can then reconstruct the image of the target if desired. This reconstructed image can be further recognized by a rotation- and distortion-invariant optical correlation techniques. Section 4 provides computer simulations of the ideas presented in Sec. 3. Finally in Sec. 5, we make some concluding remarks.

2 Recording of a Complex Hologram Using Optical Scanning Holography

A complex hologram of a 3-D target can be achieved using optical heterodyne scanning.[16–20] A rigorous mathematical analysis of the optical heterodyne scanning holographic recording technique based on a spatial-frequency domain analysis has already been described.[18] In what follows, we present only a brief and intuitive description of the technique. Figure 1 shows the optical heterodyne scanning sys-

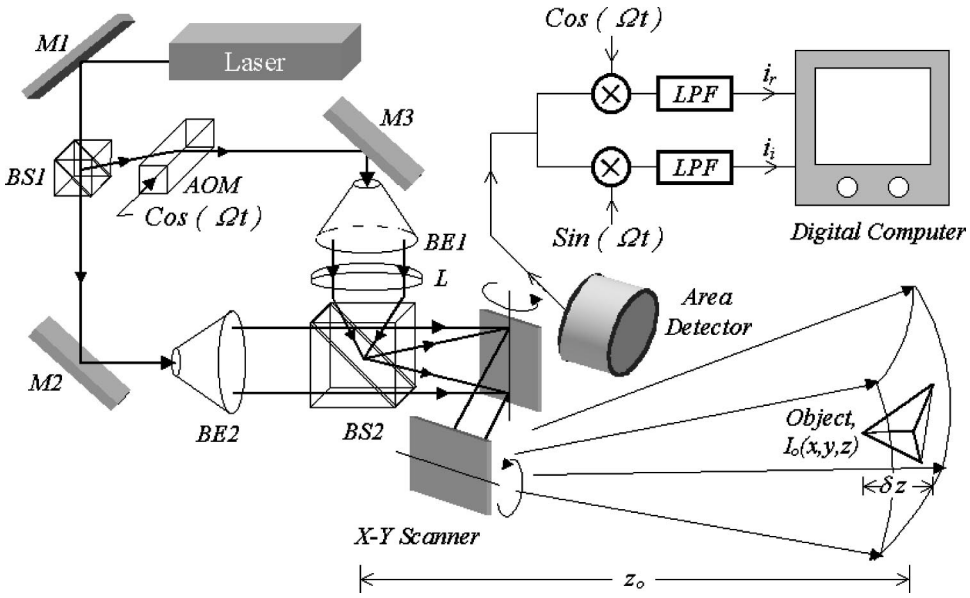

Fig. 1 Optical heterodyne scanning holographic system (*M*'s, mirrors; AOFS, acousto-optic frequency shifter, BS1 and BS2, beamsplitters; BE1 and BE2, beam expanders; *L*, focusing lens; ⊗'s, electronic multiplier; LPF, low-pass filter).

tem used to record the complex hologram of a 3-D target. In Fig. 1, the laser beam is split into two paths by beamsplitter BS1. The temporal frequency of the upper path beam is shifted by an acousto-optic frequency shifter, operating at frequency Ω. This upper path beam is collimated by a beam expander BE1. Lens L provides a spherical wave after beamsplitter BS2. This generates a temporal-frequency-shifted spherical wave of finite extent. Now, the lower path beam is collimated by beam expander BE2. This generates a plane wave of finite extent at beamsplitter BS2. The upper and lower path beams are then combined by beamsplitter BS2. The interference of the temporal-frequency-shifted spherical wave and the plane wave, both of limited extent, creates a temporally modulated Fresnel zone pattern. This Fresnel zone pattern is also limited in extent and is characterized by a numerical aperture (NA) that is the inverse sine of the half-cone angle sustained by the pattern.[19,20] The radius of the pattern at a distance z from the focal point of the spherical wave is $a(z) = (\mathrm{NA})z$. The Fresnel number of the pattern, that is the number of Fresnel zones in the pattern, is given by $F(z) = a^2(z)/\lambda z$, where λ is the wavelength of the light. Thus, the intensity of the scanning beam pattern that is the interference pattern between the temporal frequency shifted spherical wave and the plane wave of limited extent, is given by

$$I_s(x,y,z,t) = A_0(x,y)\left|1+\frac{j}{\lambda z}\exp\left[-j\,\frac{\pi}{\lambda z}(x^2+y^2)+j\Omega t\right]\right|^2, \quad (1)$$

where $A_0(x,y)$ is the size-limiting factor that is determined by the numerical aperture of the interfering beams. Here it is represented by a Gaussian envelope with radius a_0, i.e., $A_0(x,y) = \exp[-(\pi/a_0^2)(x^2+y^2)]$, and z is a depth parameter measured away from the focal point of the spherical wave.

This pattern $I_s(x,y,z,t)$ now scans the target $I_0(x,y,z)$, as shown in Fig. 1. The total intensity reflected from the target is proportional to and given by

$$\begin{aligned} I(x,y,t) &= \int\int\int I_s(x',y',z,t) \\ &\quad \times I_0(x+x',\, y+y',\, z)\,\mathrm{d}x'\,\mathrm{d}y'\mathrm{d}z \\ &= \int_{z_0-(1/2)\delta z}^{z_0+(1/2)\delta z} I_s(x,y,z,t)\odot I_0(x,y,z)\,\mathrm{d}z, \end{aligned} \quad (2)$$

where z_0 is the average distance between the target and the focal point of the spherical wave, and δz is the depth of the target. Note that the total intensity that is reflected from the target is proportional to the correlation between the scanning beam and the target's intensity. The symbol $\odot$ in Eq. (2) denotes the 2-D correlation operation that is defined as

$$\begin{aligned} g(x,y)\odot h(x,y) &= \int\int g^*(x',y') \\ &\quad \times h(x+x',\, y+y')\,\mathrm{d}x'\,\mathrm{d}y'. \end{aligned} \quad (3)$$

The total intensity is then collected and transformed to an electric signal by an area-integrating photodetector. The current output from the photodetector consists of a dc term and a heterodyne term with temporal frequency at Ω.

The in-phase and the quadrature-phase components of the heterodyne term of the output current are extracted by respectively multiplying it with $\cos(\Omega t)$ and $\sin(\Omega t)$, and

low-pass filtering. The two outputs respectively represent the correlation between the sine and cosine Fresnel zone plate (FZP) and the target's intensity[10]:

$$i_r(x,y)=\int_{z_0-(1/2)\delta z}^{z_0+(1/2)\delta z}\frac{A_0(x,y)}{\lambda z}\times\sin\left[\frac{\pi}{\lambda z}(x^2+y^2)\right]\odot I_0(x,y,z)\,\mathrm{d}z, \tag{4a}$$

$$i_i(x,y)=\int_{z_0-(1/2)\delta z}^{z_0+(1/2)\delta z}\frac{A_0(x,y)}{\lambda z}\times\cos\left[\frac{\pi}{\lambda z}(x^2+y^2)\right]\odot I_0(x,y,z)\mathrm{d}z. \tag{4b}$$

These output currents $i_r(x,y)$ and $i_i(x,y)$, when displayed on a 2-D monitor, are called the sine FZP hologram and the cosine FZP hologram of the target I_0. Alternatively, these output currents, as shown in Fig. 1, can be stored in a digital computer using an analog-to-digital converter. In the digital computer, we can construct a complex hologram, $H^c(x,y)$, by adding the two outputs in the following manner:

$$\begin{aligned}H^c(x,y)&=i_r(x,y,z)-ji_i(x,y,z)\\&=\int_{z_0-(1/2)\delta z}^{z_0+(1/2)\delta z}\frac{-jA_0(x,y)}{\lambda z}\times\exp\left[j\frac{\pi}{\lambda z}(x^2+y^2)\right]\odot I_0(x,y,z)\,\mathrm{d}z\\&=\int_{z_0-(1/2)\delta z}^{z_0+(1/2)\delta z}I_0(x,y,z)\otimes h_z(x,y)\,\mathrm{d}z,\end{aligned} \tag{5}$$

where $h_z(x,y)=[jA_0(x,y)]/(\lambda z)\exp[-j(\pi/\lambda z)(x^2+y^2)]$, to within a phase constant, is the free-space propagation impulse response.[21] The complex resulting hologram is a single-sideband hologram as it does not contain the twin-image information.[17] The symbol $\otimes$ in Eq. (5) denotes the 2-D convolution operation defined as

$$g_1(x,y)\otimes g_2(x,y)=\int\int g_1(x',y')\times g_2(x-x',y-y')\,\mathrm{d}x'\,\mathrm{d}y'. \tag{6}$$

As is commonly the situation in optical remote sensing, the target is located farther than the Rayleigh range of the scanning beam and the depth of the target is smaller than the Rayleigh range, and hence the radius and the Fresnel number of the scanning beam pattern are approximately constant within the scanned volume of the target, i.e., $a(z)\sim a_0=(\mathrm{NA})z_0$; $F(z)\sim F=a_0^2/\lambda z_0$. As a result, the free-space impulse response $h_z(x,y)$ is approximately constant within the scanned volume of the target, i.e., $h_z(x,y)\sim h_{z_0}(x,y)=[jA_0(x,y)]/(\lambda z_0)\exp[-j(\pi/\lambda z_0)(x^2+y^2)]$. Under these conditions the complex hologram of the target [see Eq. (5)] is approximated given by

$$\begin{aligned}H^c(x,y)&=\int_{z_0-(1/2)\delta z}^{z_0+(1/2)\delta z}I_0(x,y,z)\otimes h_z(x,y)\,\mathrm{d}z\\&\sim\left[\int_{z_0-(1/2)\delta z}^{z_0+(1/2)\delta z}I_0(x,y,z)\,\mathrm{d}z\right]\otimes h_{z_0}(x,y).\end{aligned} \tag{7}$$

3 Real-Only Spectrum Hologram, Depth Extraction, and Image Reconstruction

3.1 *Real-Only Spectrum Hologram*

In this subsection, we describe an algorithm that synthesizes the so-called real-only spectrum hologram, as discussed in the introduction.

According to the approximations made to obtain the results in Eq. (7), the sine FZP hologram and the cosine FZP hologram respectively are now given by

$$\begin{aligned}H_s&=\mathrm{Re}(H^c)\\&=\left[\int_{z_0-(1/2)\delta z}^{z_0+(1/2)\delta z}I_0(x,y,z)\,\mathrm{d}z\right]\otimes\left\{\frac{A_0(x,y)}{\lambda z_0}\sin\left[\frac{\pi}{\lambda z_0}(x^2+y^2)\right]\right\},\end{aligned} \tag{8a}$$

$$\begin{aligned}H_c&=\mathrm{Im}(H^c)\\&=\left[\int_{z_0-(1/2)\delta z}^{z_0+(1/2)\delta z}I_0(x,y,z)\,\mathrm{d}z\right]\otimes\left\{\frac{A_0(x,y)}{\lambda z_0}\cos\left[\frac{\pi}{\lambda z_0}(x^2+y^2)\right]\right\},\end{aligned} \tag{8b}$$

where $\mathrm{Re}(\cdot)$ and $\mathrm{Im}(\cdot)$ represents the real part and the imaginary part of Eq. (7). The spectrum of the sine and that of the cosine holograms of the target $I_0(x,y,z)$ are obtained by the Fourier transformation of Eqs. (8). The Fourier transform operation. $\mathcal{F}(\cdot)$ is defined as $\mathcal{F}\{u(x,y)\}_{k_x,k_y}=\int\int u(x,y)\exp(jk_xx+jk_yy)\mathrm{d}x\mathrm{d}y=\boldsymbol{u}(k_x,k_y)$ with k_x and k_y denoting spatial frequencies.[21] Note that the bold letter $\boldsymbol{u}$ represents the Fourier transform of u. After some manipulations, the Fourier transforms of Eqs. (8a) and (8b) are given by:

$$\begin{aligned}\boldsymbol{H_s}(k_x,k_y)&=\mathcal{F}\left[\int_{z_0-(1/2)\delta z}^{z_0+(1/2)\delta z}I_0(x,y,z)\mathrm{d}z\right]\times\mathcal{F}\left\{\frac{A_0(x,y)}{\lambda z_0}\sin\left[\frac{\pi}{\lambda z_0}(x^2+y^2)\right]\right\}\\&=\boldsymbol{I}_0(k_x,k_y)\left\{\boldsymbol{A}_0(k_x,k_y)\sin\left[\frac{\lambda z_0}{4\pi}(k_x^2+k_y^2)\right]\right\},\end{aligned} \tag{9a}$$

$$\boldsymbol{H}_c(k_x,k_y)=\mathcal{F}\left[\int_{z_0-(1/2)\delta z}^{z_0+(1/2)\delta z} I_0(x,y,z)\,\mathrm{d}z\right]\times\mathcal{F}\left\{\frac{A_0(x,y)}{\lambda z_0}\cos\left[\frac{\pi}{\lambda z_0}(x^2+y^2)\right]\right\}=\boldsymbol{I}_0(k_x,k_y)\left\{\boldsymbol{A}_0(k_x,k_y)\cos\left[\frac{\lambda z_0}{4\pi}(k_x^2+k_y^2)\right]\right\},\tag{9b}$$

where $\boldsymbol{I}_0(k_x,k_y)$ represents the Fourier transform of the target, $\boldsymbol{I}_0(k_x,k_y)=\mathcal{F}\{\int_{z_0-(1/2)\delta z}^{z_0+(1/2)\delta z} I_0(x,y,z)\mathrm{d}z\}$, and $\boldsymbol{A}_0(k_x,k_y)$, is the size limiting factor caused by the finite size of the scanning beam, given approximately by $\boldsymbol{A}_0(k_x,k_y)\sim\exp[-(1/4\pi)(\lambda z_0/a_0)^2(k_x^2+k_y^2)]$. Note that $\boldsymbol{I}_0(k_x,k_y)$ is in general a complex function and the other terms in Eqs. (9), i.e., $\boldsymbol{A}_0(k_x,k_y)$, the sine FZP and the cosine FZP are real functions. Thus Eqs. (9a) and (9b) can be rewritten as complex addition of two real-only functions Re[·] and Im[·], and are given by

$$\boldsymbol{H}_s(k_x,k_y)=\mathrm{Re}[\boldsymbol{I}_0(k_x,k_y)]\times\left\{\boldsymbol{A}_0(k_x,k_y)\sin\left[\frac{\lambda z_0}{4\pi}(k_x^2+k_y^2)\right]\right\}+j\,\mathrm{Im}[\boldsymbol{I}_0(k_x,k_y)]\times\left\{\boldsymbol{A}_0(k_x,k_y)\sin\left[\frac{\lambda z_0}{4\pi}(k_x^2+k_y^2)\right]\right\},\tag{10a}$$

$$\boldsymbol{H}_c(k_x,k_y)=\mathrm{Re}[\boldsymbol{I}_0(k_x,k_y)]\times\left\{\boldsymbol{A}_0(k_x,k_y)\cos\left[\frac{\lambda z_0}{4\pi}(k_x^2+k_y^2)\right]\right\}+j\,\mathrm{Im}[\boldsymbol{I}_0(k_x,k_y)]\times\left\{\boldsymbol{A}_0(k_x,k_y)\cos\left[\frac{\lambda z_0}{4\pi}(k_x^2+k_y^2)\right]\right\}.\tag{10b}$$

We now synthesize a hologram by adding the real parts of Eqs. (10a) and (10b) in a complex manner:

$$\boldsymbol{H}_{\text{r-only}}(k_x,k_y)=\mathrm{Re}[\boldsymbol{I}_0(k_x,k_y)]\times\left\{\boldsymbol{A}_0(k_x,k_y)\cos\left[\frac{\lambda z_0}{4\pi}(k_x^2+k_y^2)\right]\right\}+j\,\mathrm{Re}[\boldsymbol{I}_0(k_x,k_y)]\times\left\{\boldsymbol{A}_0(k_x,k_y)\sin\left[\frac{\lambda z_0}{4\pi}(k_x^2+k_y^2)\right]\right\}=\mathrm{Re}[\boldsymbol{I}_0(k_x,k_y)]\times\left\{\boldsymbol{A}_0(k_x,k_y)\exp\left[j\frac{\lambda z_0}{4\pi}(k_x^2+k_y^2)\right]\right\}.\tag{11}$$

The resulting holographic information (in the frequency domain), $\boldsymbol{H}_{\text{r-only}}(k_x,k_y)$, is called a real-only spectrum hologram. The reason is that $\boldsymbol{H}_{\text{r-only}}(k_x,k_y)$ contains the real-only information of the target's spectrum and at the same time it contains the depth information. Note that from the complex exponential term of Eq. (11) we can determine the depth location z_0 of the target. Figure 2 shows a flow chart and its first three blocks illustrate the procedures discussed so far. The inputs $i_r(x,y)$ and $i_i(x,y)$ are basically proportional to holograms H_s and H_c given by Eqs. (8). After Fourier transforming the holograms, extracting their real-only parts, and finally adding their real-only parts in a complex manner, we end up with the real-only spectrum hologram, $\boldsymbol{H}_{\text{r-only}}(k_x,k_y)$, given by Eq. (11). In the next

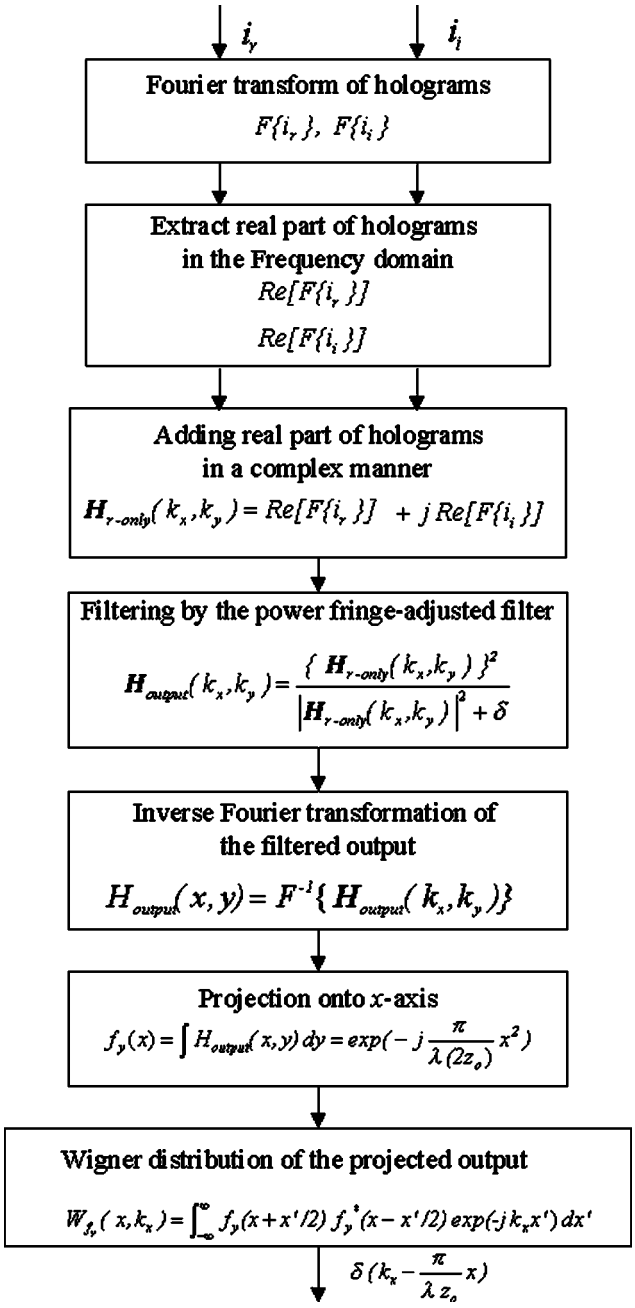

Fig. 2 Flow chart for detecting depth location of a target object from its holographic input information i_r and i_i.

subsection, we discuss a digital filtering technique to extract the depth location of the target from the real-only spectrum hologram.

3.2 *Depth Extraction from the Real-Only Spectrum Hologram*

Since the complex exponential of the real-only spectrum hologram contains the depth information of the target object as a form of fringe pattern, our goal now is to extract that piece of information. We extract the information from $\boldsymbol{H}_{\text{r-only}}(k_x,k_y)$ by applying the following power fringe-adjusted filter[10,14,15]:

$$\boldsymbol{F}(k_x,k_y)=\frac{1}{|\boldsymbol{H}_{\text{r-only}}(k_x,k_y)|^2+\delta}=\frac{1}{\{\text{Re}[\boldsymbol{I}_0(k_x,k_y)]\boldsymbol{A}_0(k_x,k_y)\}^2+\delta}, \tag{12}$$

where δ is a small value of either a constant or, some function of k_x or k_y; δ is added to overcome the possible pole problems of the filter.[14,15] Note that the denominator term, $|\boldsymbol{H}_{\text{r-only}}(k_x,k_y)|^2+\delta$, in the filter does not contain the depth information of the object because the depth information is contained only in the complex exponential of the hologram. The filtered output in the frequency domain is given by the product of the real-only spectrum hologram squared and the filter.[10,14,15] Thus the output is given by

$$\begin{aligned}\boldsymbol{H}_{\text{output}}(k_x,k_y)&=\frac{1}{|\boldsymbol{H}_{\text{r-only}}(k_x,k_y)|^2+\delta}\times[\boldsymbol{H}_{\text{r-only}}(k_x,k_y)]^2\\&=\frac{\{\text{Re}[\boldsymbol{I}_0(k_x,k_y)]\mathbf{A}_0(k_x,k_y)\}^2\exp[j(\lambda z_0/2\pi)(k_x^2+k_y^2)]}{\{\text{Re}[\boldsymbol{I}_0(k_x,k_y)]\boldsymbol{A}_0(k_x,k_y)\}^2+\delta}\\&\simeq\exp\left[j\frac{\lambda z_0}{2\pi}(k_x^2+k_y^2)\right].\end{aligned} \tag{13}$$

Note that the filtered output in the space domain is the Fresnel zone pattern located at $z=2z_0$. That is given by the inverse Fourier transformation of Eq. (13):

$$H_{\text{output}}(x,y)=\mathcal{F}^{-1}[\boldsymbol{H}_{\text{output}}(k_x,k_y)]\simeq\exp\left[-j\frac{\pi}{\lambda(2z_0)}(x^2+y^2)\right]. \tag{14}$$

Equation (14) shows that the depth location of the target is contained in the local frequency variations of the filtered output, which can be obtained from its Wigner distribution.[10,22,23] Thus, the depth location of the target can be found using the following algorithm. First, the filtered output signal is projected on the x axis. That is given by

$$\begin{aligned}f_y(x)&=\int H_{\text{output}}(x,y)\,\mathrm{d}y\\&=\int\exp\left[-j\frac{\pi}{\lambda(2z_0)}(x^2+y^2)\right]\mathrm{d}y\\&\propto\exp\left[-j\frac{\pi}{\lambda(2z_0)}x^2\right].\end{aligned} \tag{15}$$

We then calculate the Wigner distribution of Eq. (15):

$$\begin{aligned}W_{f_y}(x,k_x)&=\int f_y\left(x+\frac{x'}{2}\right)f_y^*\left(x-\frac{x'}{2}\right)\exp(-jk_xx')\,\mathrm{d}x'\\&\propto\delta\left(k_x-\frac{\pi}{\lambda z_0}x\right).\end{aligned} \tag{16}$$

Equation (16) is a line impulse with a slope $\mathrm{d}k_x/\mathrm{d}x=\pi/\lambda z_0$ on the space-frequency map ($x-k_x$ plane). Since the slope of the line delta is inversely proportional to the depth location of the object ($\mathrm{d}k_x/\mathrm{d}x=\pi/\lambda z_0$), if the wavelength is known, the depth location is found by directly measuring the slope of the line. The last three blocks of the flow chart shown in Fig. 2 summarize the procedures. We have just now extracted the depth information from the two holographic inputs $i_r(x,y)$ and $i_i(x,y)$, which are obtained from the photodetector's currents.

3.3 *Reconstruction of the Image at Its Original Depth Location*

In Sec. 3.2, we discussed the detection of the depth location of the target from its complex hologram obtained by optical scanning holography. Using the detected depth location of the target, we can reconstruct the image of the target at its original depth location. The reconstruction of the image is achieved by the convolution between the complex hologram of the target and the complex conjugate of the free-space impulse response at the depth location. Mathematically, that is given by

$$\begin{aligned}O(x,y)&=H^c(x,y)\otimes h^*_{z_0}(x,y)\\&=\left\{\int_{z_0-(1/2)\delta z}^{z_0+(1/2)\delta z}I_0(x,y,z)\,\mathrm{d}z\right\}\otimes h_{z_0}(x,y)\otimes h^*_{z_0}(x,y)\\&\propto\int_{z_0-(1/2)\delta z}^{z_0+(1/2)\delta z}I_0(x,y,z)\,\mathrm{d}z.\end{aligned} \tag{17}$$

Note that the reconstructed image is the original image of the target at its depth location. If one desires, we can now recognize the reconstructed image using conventional optical correlators, and the output of the optical correlator gives the transverse location of the matched target. In particular, for a rotated and distorted target (such as scale change), we can apply rotation- and scale-invariant optical correlation techniques.[14,15] Therefore, this makes it possible to achieve rotation- and scale-invariant recognition, and at the same time obtain the 3-D location of the target in 3-D space.

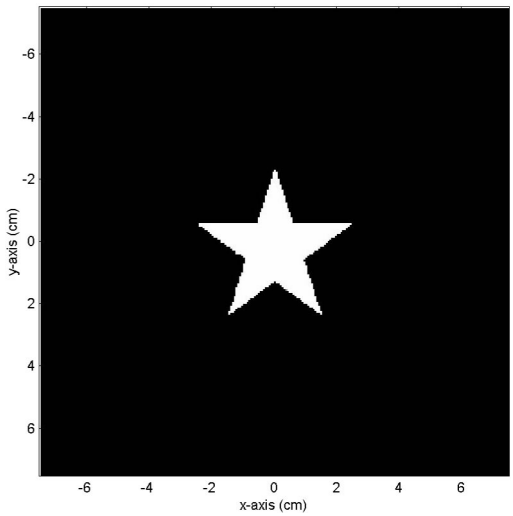

Fig. 3 Original target at a distance of 95 m from the focal point of the spherical wave projecting the scanning pattern.

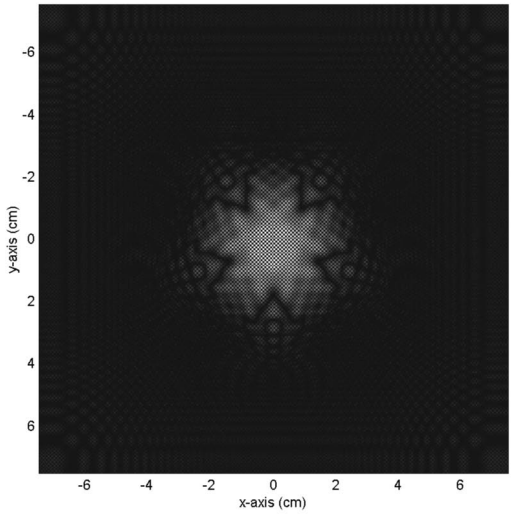

(a)

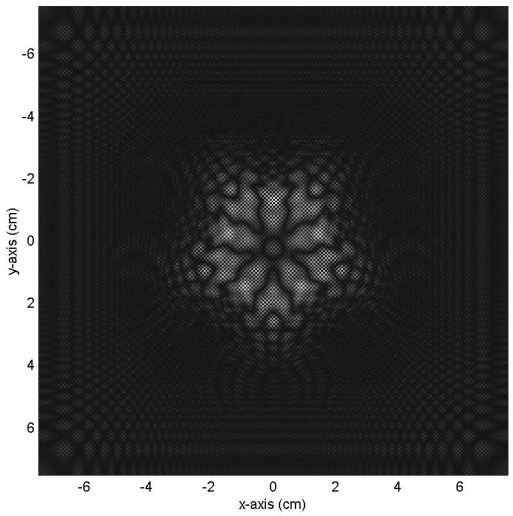

(b)

Fig. 4 (a) Cosine and (b) sine FZP holograms of the target.

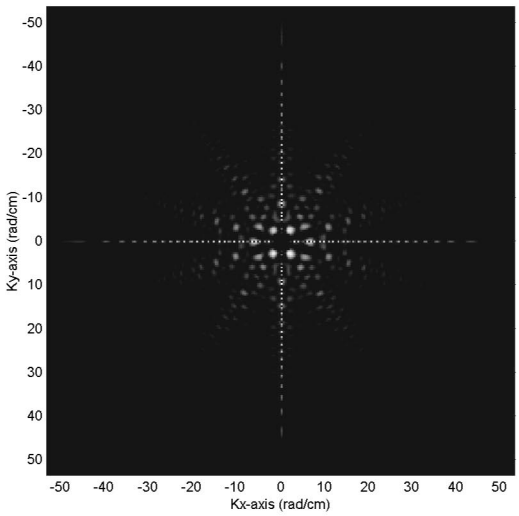

(a)

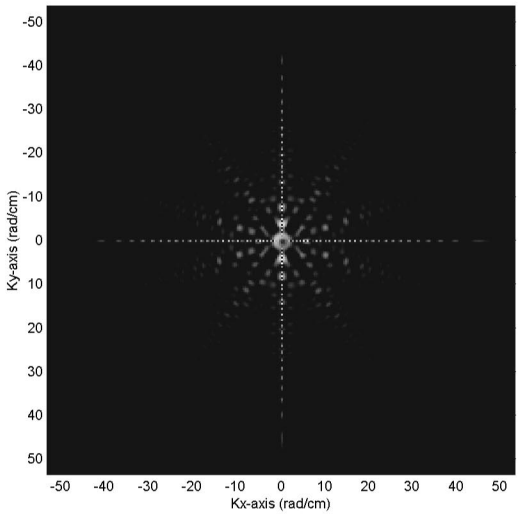

(b)

Fig. 5 (a) Real and (b) imaginary parts of the real-only spectrum hologram.

4 Computer Simulation Results

The parameters in this simulation are representative of an optical remote sensing situation where a 3-D target whose depth is smaller than the Rayleigh range of the scanning beam, is located further than the Rayleigh range. Figure (3) shows a 5-$\times$5-cm target, $O(x,y,z)$, in a 15-$\times$15-cm field of view. The target is located at a distance $z_0=95$ m from the focal point of the spherical wave projecting the scanning pattern. The radius of the scanning beam pattern is $a_0=8$ cm, at the location of the target. The numerical aperture of the scanning pattern is thus given by $\mathrm{NA}=a_0/z_0=8.42\times10^{-4}$. The wavelength of the scanning beam is $\lambda=10^{-4}$ cm. The NA and the wavelength of the scanning beam determine the Rayleigh range of the scanning beam pattern, that is given by $\lambda/(\mathrm{NA})^2=141$ cm.

Figures 4(a) and 4(b) show the cosine and sine holograms [Eq. (8) with $z_0=95$ m] that are achieved by 2-D

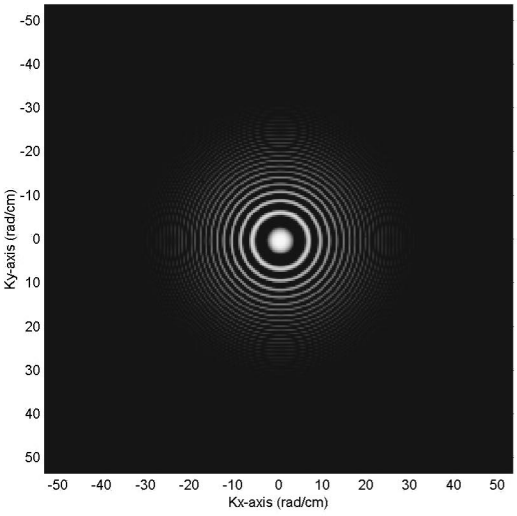

(a)

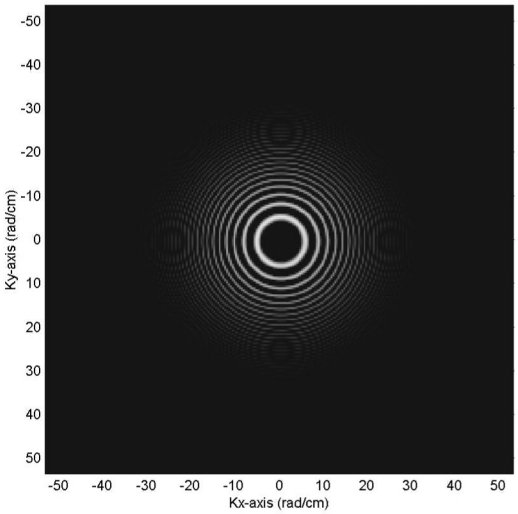

(b)

Fig. 6 (a) Real and (b) imaginary parts of filtered output.

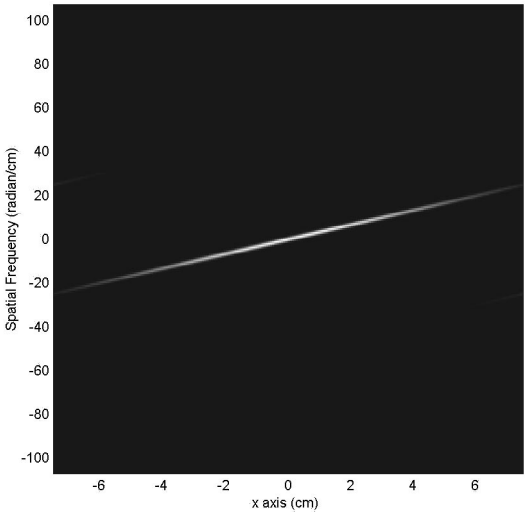

Fig. 7 Wigner distribution of filtered output.

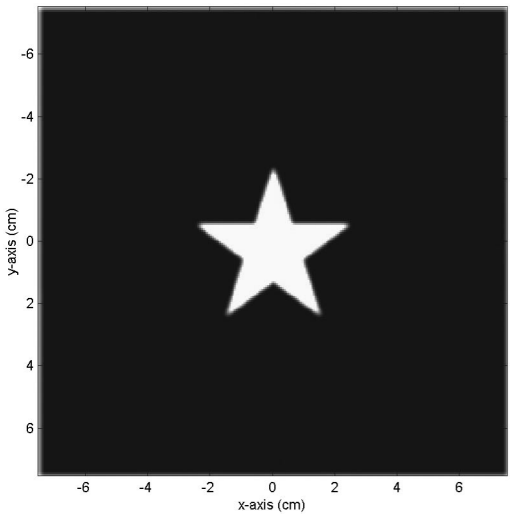

Fig. 8 Reconstructed image of the target.

scanning of the target. Again, our goal is to extract the depth information from these holograms. Figures 5(a) and 5(b) show the real and imaginary parts of the real-only spectrum hologram given by Eq. (11) and Figs. 6(a) and 6(b) show the real and imaginary parts of the filtered output given by Eq. (14). The Wigner distribution of the filtered output along the x axis is shown in Fig. 7. The slope of the line impulse gives $z_0 = 95$ m, i.e., the depth location of the target as expected. Finally, once the depth location is found, the reconstructed image of the hologram can be calculated by Eq. (17). The image is shown in Fig. 8.

5 Conclusion

We proposed a technique that extracts the depth location of a target directly from its complex hologram. The complex hologram of the target is obtained using optical scanning holography. The image of the target at its depth location is then reconstructed using the information of the depth location. One of the immediate applications of the proposed technique is rotation- and scale-invariant 3-D pattern recognition as the reconstructed image of the target can be recognized by conventional 2-D rotation- and scale-invariant optical correlation techniques.

Acknowledgments

We appreciate the support of the National Science Foundation (ECS-9810158) and Korea Research Foundation Grant (KRF-2001-003-E00145).

References

1. A. B. VanderLugt, ''Signal detection by complex spatial filtering,'' *IEEE Trans. Inf. Theory* **IT-10**, 139–145 (1964).
2. E. C. Tam, F. T. S. Yu, D. A. Gregory, and R. D. Juday, ''Autonomous real-time object tracking with an adaptive joint transform correlator,'' *Opt. Eng.* **29**, 314–320 (1990).
3. C. S. Weaver and J. W. Goodman, ''A technique for optically convolving two functions,'' *Appl. Opt.* **5**, 1248–1249 (1966).
4. N. Collings, *Optical Pattern Recognition using Holographic Techniques*, Addison-Wesley, Wokingham, England (1988).
5. G. I. Vasilenko and L. M. Tsibul'kin, *Image Recognition by Holography*, Plenum, New York (1989).
6. J. Hofer-Alfeis and R. Bamler, ''Three- and four-dimensional convolution by coherent optical filtering,'' in *Transformations in Optical*

Signal Processing, W. T. Rhodes, J. R. Fienup, and B. E. A. Saleh, Eds., *Proc. SPIE* **373**, 77–87 (1981).
7. Y. B. Karasik, ''Evaluation of three-dimensional convolutions by use of two-dimensional filtering,'' *Appl. Opt.* **36**, 7397–7401 (1997).
8. J. Rosen, ''Three-dimensional electro-optical correlation,'' *J. Opt. Soc. Am. A* **15**, 430–436 (1998).
9. T.-C. Poon and T. Kim, ''Optical image recognition of three-dimensional objects,'' *Appl. Opt.* **38**, 370–381 (1999).
10. T. Kim and T.-C. Poon, ''Extraction of 3-D location of matched 3-D object using power fringe-adjusted filtering and Wigner analysis,'' *Opt. Eng.* **38**, 2176–2183 (1999).
11. T. Kim, T.-C. Poon, M. H. Wu, K. Shinoda, and Y. Suzuki, ''Three-dimensional image matching using two-dimensional optical heterodyne scanning,'' *Opt. Mem. Neural Networks* **8**(3), 139–145 (1999).
12. T. Kim and T.-C. Poon, ''Three-dimensional matching using phase-only holographic information and Wigner distribution,'' *J. Opt. Soc. Am. A* **17**, 2520–2528 (2000).
13. M. A. Karim and M. S. Alam, Eds., Special Issue on ''Advances in Recognition Technique,'' *Opt. Eng.* (Jan. 1998).
14. X. W. Chen, Mohammad A. Karim, and M. S. Alam, ''Distortion-invariant fractional power fringe adjusted joint transform correlation,'' *Opt. Eng.* **37**, 138–143 (1998).
15. M. S. Alam, X.-W. Chen, and M. A. Karim, ''Distortion-invariant fringe-adjusted joint transform correlation,'' *Appl. Opt.* **36**, 7422–7427 (1997).
16. T.-C. Poon, M. Wu, K. Shinoda, and Y. Suzuki, ''Optical scanning holography,'' *Proc. IEEE* **84**, 753–764 (1996).
17. T.-C. Poon, T. Kim, G. Indebetouw, M. H. Wu, K. Shinoda, and Y. Suzuki, ''Twin-image elimination experiments for three-dimensional images in optical scanning holography,'' *Opt. Lett.* **25**, 215–217 (2000).
18. T.-C. Poon, ''Scanning holography and two-dimensional image processing by acousto-optic two-pupil synthesis,'' *J. Opt. Soc. Am. A* **2**(4), 521–527 (1985).
19. G. Indebetouw, P. Klysubun, T. Kim, and T.-C. Poon, ''Imaging properties of scanning holographic microscopy,'' *J. Opt. Soc. Am. A* **17**, 380–390 (2000).
20. P. Klysubun, G. Indebetouw, T. Kim, and T.-C. Poon, ''Accuracy of three-dimensional remote target location using scanning holographic correlation,'' *Opt. Commun.* **184**, 357–366 (2000).
21. T.-C. Poon and P. P. Banerjee, *Contemporary Optical Image Processing with MATLAB*, Elsevier, Oxford, England (2001).
22. T. A. C. M. Claasen and W. F. G. Mecklenbrauker, ''The Wigner distribution—a tool for time-frequency signal analysis. Part 1: Continuous-time signals,'' *Philips J. Res.* **35**, 217–250 (1980).
23. T. A. C. M. Claasen and W. F. G. Mecklenbrauker, ''The Wigner distribution—a tool for time-frequency signal analysis. Part 2: Discrete-time signals,'' *Philips J. Res.* **35**, 276–300 (1980).

Taegeun Kim received his BE degree in electronic engineering from the Kyung Hee University, Korea, in 1996 and his MS and PhD degrees in electrical engineering from Virginia Polytechnic Institute and State University in 1997 and 2000, respectively. From 2000 to 2001, he was a researcher with the Samsung Advanced Institute of Technology, Korea. He is currently an assistant professor with the Department of Optical Engineering, Sejong University, Korea. His research interests include 3-D imaging, holography, optical pattern recognition, biometric authentication, 3-D display, acousto/electro-optics, and digital signal processing. He is a member of the OSA and SPIE.

Ting-Chung Poon is a professor with Virginia Polytechnic Institute and State University (Virginia Tech.) in the Bradley Department of Electrical and Computer Engineering, where he also directs the Optical Image Processing Laboratory. His current research interests include acousto-optics, hybrid (optical/electronic/digital) image processing, optical scanning holography, optical recognition of 3-D objects, and 3-D microscopy. Dr. Poon is the coauthor of the textbooks *Principles of Applied Optics* (Irwin, 1991) and *Contemporary Optical Image Processing with Matlab* (Elsevier, 2001). He has served as a panelist for the National Institutes of Health (NIH) and the National Science Foundation (NSF), as guest editor of, among others, *Applied Optics* and *Optical Engineering*, and is on the editorial board of *Optics and Laser Technology*. Dr. Poon is a fellow of the OSA and SPIE and a senior member of the IEEE.

Guy Indebetouw: Biography and photograph not available.